EXACT SIMULATION AND SENSITIVITY ANALYSIS
OF MULTIPLEXING NETWORKS

J.W. Bandler, S. Daijavad and Q.J. Zhang

SOS-85-7-R2

July 1985

EXACT SIMULATION AND SENSITIVITY
ANALYSIS OF MULTIPLEXING NETWORKS

J.W. Bandler, Fellow, IEEE, S. Daijavad, Student Member, IEEE,

and Q.J. Zhang, Student Member, IEEE

Abstract

This paper presents a novel approach to the simulation and sensitivity analysis of multiplexing networks. All computations are performed efficiently utilizing the concept of forward and reverse analysis which is elegant and effective in cascaded circuit analysis. Formulas are derived for such responses as input or output reflection coefficient, common port and channel output port return losses, insertion loss, gain slope and group delay. Exact sensitivities w.r.t. all variables of interest, including frequency, are evaluated. The fundamental assumption is that the transmission matrices for the individual components of the network and their sensitivities w.r.t. possible variables inside them are available. An explicit algorithm is provided describing the details of the computational aspects of our theory. The formulas are applied to the optimal design of practical contiguous or non-contiguous band multiplexers consisting of multi-cavity filters distributed along a waveguide manifold. An example for optimizing a practical 12 channel, 12 GHz contiguous band multiplexer without dummy channels, which is the state-of-the-art structure used as the ouput multiplexer in satellite transponders, is presented.

I. INTRODUCTION

The design of contiguous band multiplexers consisting of multi-coupled cavity filters was a problem of significant theoretical interest for several years [1],[2], however, the manufacturing of such structures with more than 5 channels did not appear to be feasible. Recently, the subject has turned into an important development area in microwave engineering practice due to reports by leading manufacturers of successful production of 12 channel contiguous band multiplexers for satellite applications [3]-[6]. The employment of optimization techniques to determine the best multiplexer parameters has been an indispensable part of the design procedures reported [4]-[9]. The use of a powerful gradient-based minimax optimization technique [8]-[9] has reduced the CPU time required in the design procedure significantly.

The implementation of a gradient based optimization technique in multiplexer design requires, as a vital step, a robust and efficient algorithm for simulation and sensitivity analysis. In this paper, we present a new and elegant approach to the simulation of such responses as common port and channel output port return losses, insertion loss and group delay between source and channel output ports and their first-order sensitivities w.r.t. all network parameters and frequency. Our approach can be applied to any network in the general category of multiplexing or branched cascaded structures [10]. Each basic component of the structure is either a 2-port model or a 3-port junction and can contain variables or be constant. The fundamental requirement for the approach is that the transmission matrix description of all basic components and their derivatives, if they contain variables, are provided. This information is utilized in a systematic and efficient scheme which leads to the evaluation of various responses of the network at all ports of interest. An important feature of our approach is that the network structure is fully exploited and an effective cascaded analysis method, namely, the forward and reverse analysis method [11], [12] is extended and applied. Components of various complexity are permitted and nonideal effects such as losses

and dispersion can be directly taken into account. The approach handles contiguous and non-contiguous band designs in a unified manner.

The presentation is organized in the following way. In Section II, we describe the basic cascaded analysis approach as applied to a general branched cascaded circuit. Formulas for Thevenin equivalents, reflection coefficients and branch output voltages as well as their first- and second-order sensitivities w.r.t. design variables and frequency at any reference plane are developed. In Section III, we consider multiplexers consisting of multi-cavity filters distributed along a waveguide manifold. Transmission matrices and sensitivity expressions for typical components in a multiplexer, which are required by our approach, are tabulated. Response and sensitivity formulas, applicable in the multiplexer design, are also listed. In Section IV, an algorithm based on the theory discussed in Sections II and III is presented. Finally, in Section V, we consider a practical 12-channel 12 GHz multiplexer and apply our theory to optimize such a structure, taking into account many nonideal effects, using a gradient-based optimization procedure.

II. BRANCHED CASCADED NETWORKS

A multiplexer falls into the category of a general class of networks, namely, branched cascaded structures as shown in Fig. 1. For such structures, we develop a novel procedure to calculate the reflection coefficients at the common port and branch output ports as well as branch output voltages. Simultaneously, first- and second-order derivatives are evaluated. The approach is based on the computation of Thevenin source and impedance equivalents and their first- and second-order sensitivities w.r.t. design parameters and frequency at the ports of interest.

Models of Basic Components

Although the basic components of a branched cascaded circuit are 2-port elements or 3-port junctions, internally they can be complicated subnetworks characterized by

admittance, impedance or hybrid matrices. An example of such a subnetwork is the multi-coupled cavity filter described by an impedance matrix and containing many design variables. As a prerequisite step towards using our theory, the transmission matrix for each 2-port element should be deduced either by a reduction procedure or by direct measurements. Also, if variables exist in a subnetwork, the derivative of the corresponding transmission matrix should be provided. For the 3-port junctions, however, a 3-port description in the form of an arbitrary hybrid matrix, is sufficient.

Reference Planes

Consider the branched cascaded network of Fig. 1, which consists of N sections. A typical section, e.g., the kth one, has a junction, n(k) cascaded elements of branch k and a subsection along the main cascade, as shown in Fig. 2. All reference planes in the entire network are defined uniformly and numbered consecutively beginning from the main cascade termination, which is designated reference plane 1. The source port is at reference plane $2N+2$. The termination of the kth branch is called reference plane $\tau(k)$ and the branch main cascade connection (branch input port) is reference plane $\sigma(k)$, $k=1,2,...,N$, where

$$\tau(1) = 2N+3$$
$$\sigma(k) = \tau(k) + n(k), \quad k = 1, 2, ..., N \quad (1)$$
$$\tau(k) = \sigma(k-1) + 1, \quad k = 2, 3, ..., N .$$

Reduction of Junctions to 2-port Representations

Bandler et al. [11],[12] introduced the concept of forward and reverse analysis for cascaded networks. To simplify the structure under consideration to a cascade of 2-ports for which the forward and reverse analysis is applicable, the 3-port junctions are reduced to 2-port representations.

Consider the 3-port junction shown in Fig. 3. To carry the analysis through the junction along the main cascade, we terminate port 3, e.g., by calculating the equivalent

admittance seen at this port given by $Y_3 = (-I_3)/V_3$ and represent the transmission matrix between ports 1 and 2 by **A**. The analysis can also be carried through the junction into the branch by terminating port 2, e.g., calculating $Y_2 = (-I_2)/V_2$ and denoting the transmission matrix between ports 1 and 3 by **D**.

As an example, suppose the 3-port junction is characterized by a hybrid matrix **H** such that

$$[V_1 \quad I_1 \quad I_3]^T = \mathbf{H} [V_2 \quad I_2 \quad V_3]^T, \tag{2}$$

where $\mathbf{H} = [h_{ij}]_{3\times3}$. Then $\mathbf{A} = [a_{ij}]_{2\times2}$ can be found from

$$a_{ij} = (-1)^{j-1} [h_{ij} - h_{i3} h_{3j} / (Y_3 + h_{33})]. \tag{3}$$

For various forms of hybrid matrices **H**, the 2-port representation **A** or **D** is evaluated in a similar manner using elements of **H** and the equivalent termination at port 3 or 2.

Cascaded Analysis

Having reduced the junctions to 2-port representations, the network structure between any two reference planes is transformed to a simple cascade of two-ports. Assuming that the transmission matrices for all 2-ports are given, we define the equivalent transmission matrix between reference planes i and j by

$$\mathbf{Q}_{ij} \triangleq [\mathbf{p}_{ij} \quad \mathbf{q}_{ij}] \triangleq \begin{bmatrix} A_{ij} & B_{ij} \\ C_{ij} & D_{ij} \end{bmatrix}, \tag{4}$$

where

$$\mathbf{p}_{ij} \triangleq \begin{bmatrix} A_{ij} \\ C_{ij} \end{bmatrix}, \quad \mathbf{q}_{ij} \triangleq \begin{bmatrix} B_{ij} \\ D_{ij} \end{bmatrix}. \tag{5}$$

In a forward (reverse) analysis, $\mathbf{Q}_{ij}$ is computed by initializing row vectors $\mathbf{e}_1^T$ and $\mathbf{e}_2^T$ (column vectors $\mathbf{e}_1$ and $\mathbf{e}_2$) at reference plane i(j) and successively premultiplying (postmultiplying) each transmission matrix by the resulting row (column) vector until reference plane j(i) is reached. $\mathbf{e}_1$ and $\mathbf{e}_2$ are unit vectors given by $[1 \quad 0]^T$ and $[0 \quad 1]^T$, respectively.

Let ϕ be a generic notation that can be used to represent any design variable in the network. Sensitivities of $\mathbf{Q}_{ij}$ w.r.t. any variable ϕ located between reference planes i and j are evaluated as

$$\frac{\partial \mathbf{Q}_{ij}}{\partial \phi} = \sum_{\ell \in I_\phi} \frac{\partial}{\partial \phi} (\mathbf{Q}_{ij}^\ell) \, , \tag{6}$$

where I_ϕ is an index set whose elements identify the transmission matrices containing ϕ and $\partial \mathbf{Q}_{ij}{}^\ell / \partial \phi$ is the result of a forward or reverse analysis between reference planes i and j with the ℓth matrix replaced by its derivative w.r.t. ϕ. Second-order sensitivities can be derived in a similar manner as

$$\frac{\partial^2 \mathbf{Q}_{ij}}{\partial \phi \, \partial \omega} = \sum_{\ell \in I_\phi} \sum_{m \in I_\omega} \frac{\partial^2 \mathbf{Q}_{ij}^{\ell m}}{\partial \phi \, \partial \omega} \, , \tag{7}$$

where I_ϕ and I_ω are index sets, not necessarily disjoint, identifying those matrices which are functions of ϕ and ω. Also, we define $\partial^2 Q_{ij}{}^{\ell m}/(\partial \phi \, \partial \omega)$ as the second-order sensitivity of $\mathbf{Q}_{ij}$ as if ϕ and ω exist only in the ℓth and mth matrices, respectively.

Thevenin Equivalent Circuits and Basic Responses

To calculate the input reflection coefficient at the common port, the output reflection coefficients at the branch output ports, as well as the branch output voltages and their sensitivities in a unified manner, we employ Thevenin equivalents at the ports of interest evaluated by the method of forward and reverse analysis [11]. Denoting the Thevenin equivalent voltages and impedances at reference planes i and j by $V_S{}^i$, $Z_S{}^i$, $V_S{}^j$ and $Z_S{}^j$, we have

$$V_S^j = \frac{V_S^i}{A_{ij} + Z_S^i C_{ij}} \tag{8}$$

and

$$Z_S^j = \frac{B_{ij} + Z_S^i D_{ij}}{A_{ij} + Z_S^i C_{ij}} \, , \tag{9}$$

where reference plane i is located towards the source w.r.t. j, as shown in Fig. 4. The sensitivities are obtained as

$$(V_S^j)_\phi = \frac{(V_S^i)_\phi - [(A_{ij})_\phi + Z_S^i (C_{ij})_\phi + (Z_S^i)_\phi C_{ij}] V_S^j}{A_{ij} + Z_S^i C_{ij}} \qquad (10)$$

and

$$(Z_S^j)_\phi = \frac{[1 \quad Z_S^i](Q_{ij})_\phi \begin{bmatrix} -Z_S^j \\ 1 \end{bmatrix} + (Z_S^i)_\phi (D_{ij} - Z_S^j C_{ij})}{A_{ij} + Z_S^i C_{ij}} \;, \qquad (11)$$

where subscript ϕ denotes $\partial/\partial\phi$.

If the reflection coefficient at the kth branch output port and its sensitivities are to be calculated, then (9) and (11) are specialized to

$$Z_S^{\tau+1} = \frac{B}{A} \qquad (12)$$

and

$$(Z_S^{\tau+1})_\phi = \frac{(B)_\phi - (A)_\phi Z_S^{\tau+1}}{A} \;, \qquad (13)$$

where $A \equiv A_{2N+2,\tau+1}, B \equiv B_{2N+2,\tau+1}$ and $\tau \equiv \tau(k)$. This is simply due to the fact that there is no impedance to the left of reference plane $2N+2$, i.e., $Z_S^{2N+2} = 0$. The corresponding output reflection coefficient is defined as

$$\rho^k \triangleq \frac{Z_S^{\tau+1} - R_L^k}{Z_S^{\tau+1} + R_L^k} \;, \qquad (14)$$

where R_L^k is the load resistance at the kth channel output. Clearly, (13) is utilized in the evaluation of $(\rho^k)_\phi$ as

$$(\rho^k)_\phi = \frac{(Z_S^{\tau+1})_\phi (1 - \rho^k)}{Z_S^{\tau+1} + R_L^k} \;. \qquad (15)$$

Channel output voltage is also computed by utilizing the Thevenin equivalent voltage source and impedance at the branch output port. At the kth channel we have

$$V^k = \frac{R_L^k}{A (R_L^k + Z_S^{\tau+1})} \;, \qquad (16)$$

assuming a normalized excitation at the source port. This can be easily explained by noticing that V^k is evaluated using a voltage divider once $V_S^{\tau+1}$ is known. Using (8) and taking into account that $V_S^{2N+2} = 1$ and $Z_S^{2N+2} = 0$, we have $V_S^{\tau+1} = 1/A$. Also

$$(V^k)_\phi = -R_L^k V^k \left[\frac{(A)_\phi}{A} + \frac{(Z_S^{\tau+1})_\phi}{R_L^k + Z_S^{\tau+1}} \right]. \tag{17}$$

The second-order sensitivity of V^k w.r.t. ϕ and ω, i.e., $\partial^2 V^k/(\partial\phi\partial\omega)$ is obtained via evaluation of $\partial^2 Z_S^{\tau+1}/(\partial\phi\,\partial\omega)$. Substituting ω for ϕ in (13) and differentiating w.r.t. ϕ, gives

$$(Z_S^{\tau+1})_{\phi\omega} = \frac{(B)_{\phi\omega} - Z_S^{\tau+1}(A)_{\phi\omega} - (A)_\omega(Z_S^{\tau+1})_\phi - (Z_S^{\tau+1})_\omega(A)_\phi}{A}, \tag{18}$$

where double subscript $\phi\omega$ denotes $\partial^2/(\partial\phi\,\partial\omega)$.

Now, replacing ϕ by ω in (17) and differentiating w.r.t. ϕ, we have

$$(V^k)_{\phi\omega} = \frac{(V^k)_\phi(V^k)_\omega}{V^k} - R_L^k V^k \left[\frac{A(A)_{\phi\omega} - A_\phi A_\omega}{A^2} + \right.$$
$$\left. \frac{(Z_S^{\tau+1})_{\phi\omega}(R_L^k + Z_S^{\tau+1}) - (Z_S^{\tau+1})_\omega(Z_S^{\tau+1})_\phi}{(R_L^k + Z_S^{\tau+1})^2} \right] \tag{19}$$

Norton equivalent admittances and current sources are calculated similarly to the Thevenin equivalents. Denoting the Norton equivalent currents and admittances at reference planes i and j by I_L^i, Y_L^i, I_L^j and Y_L^j, we have

$$Y_L^i = \frac{C_{ij} + Y_L^j D_{ij}}{A_{ij} + Y_L^j B_{ij}} \tag{20}$$

and

$$I_L^i = I_L^j = 0. \tag{21}$$

Also,

$$(Y_L^i)_\phi = \frac{[-Y_L^i \quad 1](\mathbf{Q}_{ij})_\phi \begin{bmatrix} 1 \\ Y_L^j \end{bmatrix} + (Y_L^j)_\phi (D_{ij} - Y_L^i B_{ij})}{A_{ij} + Y_L^j B_{ij}}. \tag{22}$$

As special cases of (20), the equivalent admittances Y_3 and Y_2 required in the reduction of junctions to 2-port representations are calculated as

$$Y_3^k = Y_L^{\sigma(k)} = \frac{C_{\sigma(k), \tau(k)}}{A_{\sigma(k), \tau(k)}} \; , \quad k = 1, 2, ..., N \tag{23}$$

and, for a short-circuit main cascade termination,

$$Y_2^k = Y_L^{2k} = \frac{D_{2k,1}}{B_{2k,1}} \; , \quad k = 1, 2, ..., N \; . \tag{24}$$

The common port reflection coefficient is also computed using the Norton equivalent

(at the source reference plane) as

$$\rho^0 = 1 - \frac{2 \, R_S \, D_{2N+2,1}}{B_{2N+2,1}} \; . \tag{25}$$

Its sensitivity is given by

$$(\rho^0)_\phi = 2 \, R_S \, \frac{(B)_\phi D - (D)_\phi B}{B^2} \tag{26}$$

where $B \equiv B_{2N+2,1}$ and $D \equiv D_{2N+2,1}$.

III. ANALYSIS OF SPECIFIC MULTIPLEXER STRUCTURES

While the approach developed in Section II is general, as a special case, the design of

multiplexers consisting of coupled cavity filters distributed along a waveguide manifold is

considered here in more detail. Contiguous or non-contiguous band multiplexers are treated

in a similar manner. Fig. 5, which is a special case for the structure in Fig. 1, illustrates a

typical circuit equivalent for a multiplexer. A branch consists of a coupled-cavity filter,

together with input-output transformers, and an impedance inverter. A subsection is the

waveguide section separating two adjacent filters and the junction is the equivalent circuit

model for the physical junction between channel filters and the manifold. The main cascade is

short-circuited and the responses of interest are common port return loss, channel output

return loss, insertion or transducer loss, gain slope and group delay between common port and

channel output ports.

To apply the general method of Section II, the subnetworks, namely, channel filters,

waveguide spacings and junctions should be represented by 2-port transmission matrices.

Recently, a comprehensive set of formulas for reduction of multi-cavity filters to two-port

equivalents which also provides sensitivities w.r.t. variables of interest in the filter structure,

has been presented [13]. The formulas evaluate short-circuit admittance parameters and

their sensitivities w.r.t. all couplings as well as frequency for the unterminated filter model

and take many nonideal effects such as losses, stray couplings and dispersion into account.

Evaluation of transmission matrices from short-circuit admittance matrices is straight-

forward. Here we describe the essential information in [13] which is appropriate to this

paper.

The symmetrical impedance matrix for a narrow-band lumped model of an

unterminated filter is given by

$$\mathbf{Z} = j(s\mathbf{1} + \mathbf{M}) + r\mathbf{1} \tag{27}$$

where $\mathbf{1}$ denotes an $n \times n$ identity matrix and s is the normalized frequency variable given by

$$s \triangleq \frac{\omega_0}{\Delta\omega} \left(\frac{\omega}{\omega_0} - \frac{\omega_0}{\omega} \right), \tag{28}$$

ω_0 and $\Delta\omega$ being the synchronously tuned cavity resonant frequency and the bandwidth

parameter. We assume uniform dissipation for all cavities indicated by parameter r where

$$r = \frac{\omega_0}{\Delta\omega Q_f}, \tag{29}$$

Q_f representing the unloaded Q-factor. In equation (27), $\mathbf{M}$ is the coupling matrix whose (i, j)

element represents the normalized coupling between the ith and jth cavities and the diagonal

entries M_{ii} represent the deviations from synchronous tuning. Dispersion effects on the filter

are modelled by a frequency dependent $\mathbf{M}$ matrix. It is easy to prove [13] that to calculate the

short-circuit admittance parameters and their sensitivities w.r.t. all couplings and frequency,

we only need the solution of two systems of equations, namely,

$$\mathbf{Z}\mathbf{p} = \mathbf{e}_1 \tag{30}$$

and

$$\mathbf{Z}\mathbf{q} = \mathbf{e}_n, \tag{31}$$

where $\mathbf{e}_1 = [1 \ 0 \ldots 0]^T$ and $\mathbf{e}_n = [0 \ldots 0 \ 1]^T$.

In Table 1, the transmission matrices for the individual components of the multiplexer structure shown in Fig. 5, have been listed. The series 3-port junctions are reduced to 2-port equivalents using the method described in Section II. Table 2 lists the sensitivities of transmission matrices in Table 1 w.r.t. relevant parameters and frequency.

In Table 3, various frequency responses of interest in a multiplexer structure and their sensitivities w.r.t. design parameter ϕ have been summarized. It is clear that the evaluation of reflection coefficients at the common port and channel output ports (ρ^0 and ρ^k), channel output voltages (V^k) and the first- and second-order sensitivities

$$\left(\frac{\partial \rho^0}{\partial \phi}, \frac{\partial \rho^k}{\partial \phi}, \frac{\partial V^k}{\partial \phi}, \frac{\partial V^k}{\partial \omega} \text{ and } \frac{\partial^2 V^k}{\partial \phi \partial \omega} \right),$$

as described in Section II, is sufficient to compute all responses and sensitivities tabulated.

IV. ALGORITHM FOR CALCULATION OF THEVENIN EQUIVALENTS AND THEIR SENSITIVITIES

The following algorithm can be used to obtain Thevenin equivalents at output ports and their sensitivities w.r.t. any variable. The algorithm assumes that the transmission matrices for all 2-port elements and the hybrid matrices for all junctions, as well as their sensitivities are given. The reverse analysis along the main cascade is initialized by e_2 for a short circuit termination or, e_1 for an open circuit termination. Correspondingly, the resulting analysis is represented by q vectors (as in the algorithm) or p vectors.

Step 1 For $k = 1, 2, ..., N$, set σ and τ to $\sigma(k)$ and $\tau(k)$, respectively, and execute Steps 1.1 to 1.7.

Step 1.1 Calculate $Q_{i,\tau+1}$ by reverse analysis for $i = \tau+1, \tau+2, ..., \sigma$. Calculate $Q_{\sigma j}$ by forward analysis for $j = \sigma, \sigma-1, ..., \tau+1$.

Comment Cascaded analysis is performed on the kth branch. The reverse (forward) analysis starts from the branch output (input) port and is carried to the branch input (output) port.

Step 1.2 $\mathbf{p}_{\sigma\tau} \leftarrow \mathbf{Q}_{\sigma,\tau+1} \, \mathbf{A}_\tau \, \mathbf{e}_1.$

Calculate Y_3^k using (23).

Comment   The equivalent admittance of the kth branch, looking from the branch input

port, is computed. This admittance is utilized in the 2-port representation of

the kth junction.

Step 1.3   Calculate $\partial\mathbf{p}_{\sigma\tau}/\partial\phi$ using (6) and $\partial Y_3^k/\partial\phi$ from (22) for all the variable ϕ's in the

kth branch.

Comment   Sensitivities of the branch equivalent admittance w.r.t. all variables in the

branch are calculated. In evaluating $\partial Y_3^k/\partial\phi$, we use a special case for (22)

which corresponds to Y_3^k given in (23).

Step 1.4   Calculate $\mathbf{A}_{2k}$ using (3). Calculate $\partial\mathbf{A}_{2k}/\partial\phi$ for all the variable ϕ's in the kth

junction and the kth branch.

Comment   The 2-port representation of the kth junction, when terminating its port 3, is

computed. The sensitivities of the resulting transmission matrix are readily

obtained.

Step 1.5   Calculate $\mathbf{q}_{2k,1}$ by reverse analysis and Y_2^k from (24).

Comment   The equivalent admittance at port 2 of the kth junction, looking towards the

main cascade termination, is calculated after a reverse analysis from

reference plane 1 to reference plane 2k.

Step 1.6   Calculate $\partial\mathbf{q}_{2k,1}/\partial\phi$ using (6) and $\partial Y_2^k/\partial\phi$ using (22) for all variables ϕ in

section k', $k' < k$ and in the kth spacing.

Comment   The sensitivities of the equivalent admittance Y_2^k, w.r.t. all variables

geometrically located to the right of junction k, are computed. In evaluating

$\partial Y_2^k/\partial\phi$, we use a special case for (22) which corresponds to Y_2^k, given in (24).

Step 1.7   Calculate $\mathbf{D}_{2k}$ using the method described in Section II. Calculate $\partial\mathbf{D}_{2k}/\partial\phi$ for

all the variable ϕ's in the kth junction and spacing, as well as in all k'

sections, $k' < k$.

<u>Comment</u>	The 2-port representation of junction k when terminating its port 2, is computed. The sensitivities of the resulting transmission matrix w.r.t. all variables, included in or located to the right of the junction, are computed.
<u>Step 2</u>	Calculate $q_{2N+2,1}$ by extending the reverse analysis already performed up to reference plane 2N in Step 1.5, to reference plane $2N+2$. Note that A_{2N} has been evaluated in Step 1.4.

Calculate $\partial q_{2N+2,1}/\partial\phi$ using $\partial q_{2N,1}/\partial\phi$ (ϕ belongs to the set of all variables to the right of section N and the Nth spacing), which has been evaluated in Step 1.6 and $\partial A_{2N}/\partial\phi$ (ϕ belongs to the set of all variables in the Nth branch and Nth junction), which has been evaluated in Step 1.4.

<u>Comment</u>	The reverse analysis from the main cascade termination is carried back to the source port. The corresponding sensitivities are also calculated. These results are used to calculate the common port reflection coefficient and its sensitivities w.r.t. all variables in the entire network.
<u>Step 3</u>	For k = N, N–1, ..., 1, set σ and τ to $\sigma(k)$ and $\tau(k)$, respectively and execute Steps 3.1 to 3.3.
<u>Step 3.1</u>	Calculate $\mathbf{Q}_{2N+2,\,2k+1}$ by forward analysis.
<u>Comment</u>	The forward analysis is carried along the main cascade from the source port to the input port of junction k.
<u>Step 3.2</u>	$\mathbf{Q}_{2N+2,\,\tau+1} \leftarrow \mathbf{Q}_{2N+2,\,2k+1}\,\mathbf{D}_{2k}\,\mathbf{Q}_{\sigma,\,\tau+1}.$

Calculate $\partial\mathbf{Q}_{2N+2,\,\tau+1}/\partial\phi$ using (6) for all the variable ϕ's in the entire multiplexer.

<u>Comment</u>	A cascaded analysis from the source port is carried through the kth junction into the kth branch. The sensitivities w.r.t. all variables are computed.
<u>Step 3.3</u>	Calculate $V_S^{\tau+1}$ and $Z_S^{\tau+1}$ using (8) and (9). Also, calculate $\partial V_S^{\tau+1}/\partial\phi$ and $\partial Z_S^{\tau+1}/\partial\phi$ using (10) and (11) for all variables ϕ in the entire multiplexer.

Comment Thevenin equivalents and their sensitivities are computed for the kth branch

      output port.

V. EXAMPLE

A wide range of possible multiplexer optimization problems can be formulated and solved by appropriately defining specifications on various frequency responses of interest. The sensitivities are used in conjunction with the gradient-based minimax algorithm of Hald and Madsen [14] to ensure the fastest possible solutions.

As an example, we have used our simulation and sensitivity formulas to optimize a 12-channel, 12 GHz multiplexer without dummy channels. Waveguide spacings, input and output transformer ratios, cavity resonant frequencies as well as intercavity couplings are used as optimization variables.

The details of the problem are as follows. There are twelve 6th-order multi-cavity filters mounted on the waveguide manifold. The transmission matrix deduced from the commonly used impedance matrix description of these filters has been formulated in Table 1. An optimization on a singly terminated filter was performed to obtain the starting values for the non-zero couplings M_{12}, M_{23}, M_{34}, M_{36}, M_{45}, M_{56} and the same values were assumed for all filters. The unloaded Q-factor is estimated at 12000 and dispersion effects consistent with the models in use at ComDev Ltd. [15] are included. In selecting the starting values of waveguide spacings, for each section the half guide wavelength evaluated at the center frequency of the corresponding channel filter, as suggested in the literature [1], was used. The model for the nonideal junctions, i.e., the equivalent admittances Y_a and Y_c of Fig. 5, which have also been assumed in the transmission matrix description of junctions as appearing in Table 1, are consistent with the models suggested by Chen et al. [2] following the formulas by Marcuvitz [16]. Fig. 6 shows the common port return loss and channel insertion loss responses at the starting point for the optimization of the whole structure.

The specific optimization problem considered in this example was to satisfy a lower specification of 20 dB on the common port return loss over the entire frequency band of interest for the multiplexer. From Table 3 it is clear that the evaluation of common port return loss and its sensitivities w.r.t. the generic optimization variable ϕ is straight-forward once the common port reflection coefficient ρ^o and its sensitivities $(\rho^o)_\phi$ are known. We will describe the particular variables considered in this example later. Recalling equations (25) and (26) and the definition of q_{ij} in (5), ρ^o and $(\rho^o)_\phi$ are evaluated from $q_{2N+2,1}$ and its sensitivities. Finally, by referring to the algorithm and specifically Step 2 in this case, $q_{2N+2,1}, \partial q_{2N+2,1}/\partial\phi$ are calculated.

The optimization was performed in several stages with the judicious addition of new variables at each stage to improve the overall response or the response over some specific portions of the total frequency band. In particular, the first stage was the optimization w.r.t. only waveguide spacings, i.e., 12 variables, and the last stage involved 60 variables, namely, 12 section lengths, 14 variables for each of channels 1 and 12 (all 6 possible intercavity couplings, 6 cavity resonant frequencies, input and output transformer ratios) and 4 variables for each of channels 2, 8, 9, 10, and 11 (input and output transformer ratios, resonant frequency of the first cavity and coupling M_{12}). In selection of the frequency points, uniformly distributed points, 10 MHz apart over the whole 500 MHz band, are taken in the early stages. However, a simple interpolation technique effectively treating sample points 1 MHz apart is introduced in the final stages of the optimization. The total CPU time on the Cyber 170/815 system was about ten minutes. The results of the final optimization are shown in Fig. 7. Equi-ripple return loss response satisfying the requirements over the entire communication band has been achieved.

The results presented in this paper verify a highly efficient, state-of-the-art computer program package for simulation, sensitivity analysis and optimization of multiplexers called MXSOS2. That package was developed by Optimizations Systems Associates [17] for

ComDev Ltd. [15]. MXSOS2 was tested in close cooperation with members of ComDev Ltd., directly involved in multiplexer design and postproduction tuning [8].

VI. CONCLUSIONS

We have presented a new approach to simulation and sensitivity analysis of multiplexing networks. By utilizing our formulas of Thevenin equivalents and their sensitivities w.r.t. network parameters as well as frequency, various frequency responses and their sensitivities at arbitrarily chosen reference planes are evaluated. The method presented has been utilized in the optimal design of a state-of-the-art 12 channel contiguous band multiplexer. Attractive and fast computer results obtained using a gradient-based optimization technique justify our treatment of sensitivity evaluation as an integral part of the analysis. All the sensitivity formulas presented in this paper can be verified independently. Actual implementation of our approach, however, requires only an understanding of the definitions of the responses, formulas for which are available in Table 3. For more theoretically oriented researchers or engineers, our method of dealing with the sensitivities (Section II) is straightforward and should be applicable to almost any complex linear circuit structure in the frequency domain.

REFERENCES

[1]   A.E. Atia, "Computer-aided design of waveguide multiplexers", <u>IEEE Trans. Microwave Theory Tech.</u>, vol. MTT-22, 1974, pp. 332-336.

[2]   M.H. Chen, F. Assal and C. Mahle, "A contiguous band multiplexer", <u>COMSAT Technical Review</u>, vol. 6, 1976, pp. 285-306.

[3]   R. Tong, J. Dorey, P. Mabson, W.C. Tang, E. Klein-Lebbink and C.M. Kudsia, "An 11 GHz contiguous band output multiplexing network for Intelsat VI spacecraft", <u>1982 IEEE Int. Microwave Symp. Digest</u> (Dallas, TX, 1982), pp. 405-407.

[4]   M.H. Chen, "A 12-channel contiguous band multiplexer at KU-band", <u>1983 IEEE Int. Microwave Symp. Digest</u> (Boston, MA, 1983), pp. 77-79.

[5]   R.G. Egri, A.E. Williams and A.E. Atia, "A contiguous-band multiplexer design", <u>1983 IEEE Int. Microwave Symp. Digest</u> (Boston, MA, 1983), pp. 86-88.

[6]   S.C. Holme, "A 12 GHz 12 channel multiplexer for satellite applications", <u>1984 IEEE Int. Microwave Symp. Digest</u> (San Fransisco, CA, 1984), pp. 295-296.

[7]   M.H. Chen, "Current state-of-the-art technology on contiguous-band multiplexer", <u>Proc. IEEE Int. Symp. Circuits and Systems</u> (Kyoto, Japan, 1985), pp. 1583-1586.

[8]   J.W. Bandler, S.H. Chen, S. Daijavad and W. Kellermann, "Optimal design of multi-cavity filters and contiguous-band multiplexers", <u>Proc. 14th European Microwave Conference</u> (Liège, Belgium, 1984), pp. 863-868.

[9]   J.W. Bandler, W. Kellermann and K. Madsen, "A superlinearly convergent minimax algorithm for microwave circuit design", <u>IEEE Trans Microwave Theory Tech.</u>, to be published.

[10] J.W. Bandler, S. Daijavad and Q.J. Zhang, "Computer aided design of branched cascaded networks", <u>Proc. IEEE Int. Symp. Circuits and Systems</u> (Kyoto, Japan, 1985), pp. 1579-1582.

[11] J.W. Bandler, M.R.M. Rizk and H.L. Abdel-Malek, "New results in network simulation, sensitivity and tolerance analysis for cascaded structures", <u>IEEE Trans. Microwave Theory Tech.</u>, vol. MTT-26, 1978, pp. 963-972.

[12] J.W. Bandler and M.R.M. Rizk, "Tolerance analysis of cascaded structures", <u>IEEE Trans. Microwave Theory Tech.</u>, vol. MTT-28, 1980, pp. 935-938.

[13] J.W. Bandler, S.H. Chen and S. Daijavad, "Exact sensitivity analysis for optimization of multi-coupled cavity filters", Department of Electrical and Computer Engineering, McMaster University, Hamilton, Canada, Report SOS-85-2, 1985.

[14] J. Hald and K. Madsen, "Combined LP and quasi-Newton methods for minimax optimization", <u>Mathematical Programming</u>, vol. 20, 1981, pp. 49-62.

[15] ComDev Ltd., 155 Sheldon Drive, Cambridge, Ontario, Canada N1R 7H6, private communications, 1983-1984.

[16]   N. Marcuvitz, <u>Waveguide Handbook</u>, MIT Rad. Lab. Ser., vol. 10.   New York:
        McGraw-Hill, 1951.

[17]   Optimization Systems Associates, 163 Watson's Lane, Dundas, Ontario, Canada
        L9H 6L1, 1983-1984.

TABLE 1

EXAMPLES OF TRANSMISSION MATRICES FOR SUBNETWORKS
IN THE MULTIPLEXER OF FIG. 5

Subnetwork	Transmission Matrix	
	Expression	Notation
output transformer $n_2{:}1$	$\begin{bmatrix} n_2 & 0 \\ 0 & \dfrac{1}{n_2} \end{bmatrix}$	$\mathbf{A}$
multi-coupled cavity filter[†]	$\dfrac{1}{q_1}\begin{bmatrix} -q_n & -1 \\ q_1^2 - p_1 q_n & -p_1 \end{bmatrix}$	$\mathbf{A}$
input transformer $1{:}n_1$	$\begin{bmatrix} \dfrac{1}{n_1} & 0 \\ 0 & n_1 \end{bmatrix}$	$\mathbf{A}$
series junction terminated at port 3 by Y_3, $(Y = Y_c + Y_3)$	$\dfrac{1}{Y}\begin{bmatrix} Y + Y_a & 1 \\ 2Y_a Y + Y_a^2 & Y + Y_a \end{bmatrix}$	$\mathbf{A}$
series junction terminated at port 2 by Y_2, $(Y = Y_a + Y_2)$	$\dfrac{1}{Y}\begin{bmatrix} Y + Y_c & 1 \\ Y(Y_a + Y_c) + Y_a Y_c & Y + Y_a \end{bmatrix}$	$\mathbf{D}$
waveguide spacing[††]	$\begin{bmatrix} \cos\theta & jZ_0\sin\theta \\ \dfrac{j\sin\theta}{Z_0} & \cos\theta \end{bmatrix}$	$\mathbf{A}$

[†] $p_i(q_i)$ is the ith element of vector $\mathbf{p}(\mathbf{q})$ which is the solution of $\mathbf{Zp} = \mathbf{e}_1$ $(\mathbf{Zq} = \mathbf{e}_n)$, where $\mathbf{Z} = j(s\mathbf{1} + \mathbf{M}) + r\mathbf{1}$ and $s = (\omega_0/\Delta\omega)(\omega/\omega_0 - \omega_0/\omega)$ for a filter with coupling matrix $\mathbf{M}$ centered at ω_0 and having a bandwidth parameter $\Delta\omega$ and a uniform cavity dissipation parameter r.

[††]   a waveguide section has a characteristic impedance Z_0 and $\theta = \beta\ell$, $\beta = 2\pi/\lambda_g$, where ℓ is the section length and λ_g is the guide wavelength.

TABLE 2

FIRST-ORDER SENSITIVITIES OF THE TRANSMISSION
MATRICES IN TABLE 1

Subnetwork	Identification	Sensitivity of the Transmission Matrix
output transformer	$\dfrac{\partial \mathbf{A}}{\partial n_2}$	$\begin{bmatrix} 1 & 0 \\ 0 & -\dfrac{1}{n_2^2} \end{bmatrix}$
multi-coupled cavity filter	$\dfrac{\partial \mathbf{A}}{\partial M_{ab}}$	$\dfrac{jc^{\dagger}}{2q_1}(p_a q_b + q_a p_b)\,\mathbf{A} +$ $\dfrac{jc}{q_1}\begin{bmatrix} q_a q_b & 0 \\ p_1 q_a q_b + q_n p_a p_b - q_1(p_a q_b + p_b q_a) & p_a p_b \end{bmatrix}$
	$\dfrac{\partial \mathbf{A}}{\partial \omega}$	$\dfrac{s_\omega}{q_1}\left(\mathbf{p}^T\mathbf{q}\,\mathbf{A} + \begin{bmatrix} \mathbf{q}^T\mathbf{q} & 0 \\ p_1\mathbf{q}^T\mathbf{q} + q_n\mathbf{p}^T\mathbf{p} - 2q_1\mathbf{p}^T\mathbf{q} & \mathbf{p}^T\mathbf{p} \end{bmatrix}\right)$
input transformer	$\dfrac{\partial \mathbf{A}}{\partial n_1}$	$\begin{bmatrix} -\dfrac{1}{n_1^2} & 0 \\ 0 & 1 \end{bmatrix}$
series junction terminated at port 3 [††]	$\dfrac{\partial \mathbf{A}}{\partial \phi}\,,\ \phi \in Y_3$	$(Y_3)_\phi\,\mathbf{K}_1$
	$\dfrac{\partial \mathbf{A}}{\partial \phi}\,,\ \phi \in J$	$(Y_c)_\phi\,\mathbf{K}_1 + (Y_a)_\phi\,\mathbf{K}_2$
	$\dfrac{\partial \mathbf{A}}{\partial \omega}$	$(Y_3 + Y_c)_\omega\,\mathbf{K}_1 + (Y_a)_\omega\,\mathbf{K}_2$

TABLE 2 (continued)

Subnetwork	Identification	Sensitivity of the Transmission Matrix
series junction terminated at port 2 [†††]	$\dfrac{\partial \mathbf{D}}{\partial \phi}$, $\phi \in Y_2$	$(Y_2)_\phi \, \mathbf{L}_1$
	$\dfrac{\partial \mathbf{D}}{\partial \phi}$, $\phi \in J$	$(Y_a)_\phi \, (\mathbf{L}_1 + \mathbf{L}_2) + (Y_c)_\phi \, \mathbf{L}_3$
	$\dfrac{\partial \mathbf{D}}{\partial \omega}$	$(Y_2 + Y_a)_\omega \, \mathbf{L}_1 + (Y_a)_\omega \, \mathbf{L}_2$
		$+ \; (Y_c)_\omega \, \mathbf{L}_3$
waveguide spacing	$\dfrac{\partial \mathbf{A}}{\partial \ell}$	$\beta \begin{bmatrix} -\sin\theta & j\,Z_0\cos\theta \\ \dfrac{j\cos\theta}{Z_0} & -\sin\theta \end{bmatrix}$
	$\dfrac{\partial \mathbf{A}}{\partial \omega}$	$\ell(\beta)_\omega \begin{bmatrix} -\sin\theta & j\,Z_0\cos\theta \\ \dfrac{j\cos\theta}{Z_0} & -\sin\theta \end{bmatrix}$

[†] $c = \begin{cases} 2 \text{ if } a \neq b \\ 1 \text{ if } a = b \end{cases}$

[††] $\mathbf{K}_1 = -\dfrac{1}{Y^2} \begin{bmatrix} Y_a & 1 \\ Y_a^2 & Y_a \end{bmatrix}$, $\mathbf{K}_2 = \dfrac{1}{Y} \begin{bmatrix} 1 & 0 \\ 2(Y_a + Y) & 1 \end{bmatrix}$

[†††] $\mathbf{L}_1 = -\dfrac{1}{Y^2} \begin{bmatrix} Y_c & 1 \\ Y_a Y_c & Y_a \end{bmatrix}$, $\mathbf{L}_2 = \dfrac{1}{Y} \begin{bmatrix} 0 & 0 \\ Y_c + Y & 1 \end{bmatrix}$, $\mathbf{L}_3 = \dfrac{1}{Y} \begin{bmatrix} 1 & 0 \\ Y_a + Y & 0 \end{bmatrix}$

TABLE 3

VARIOUS FREQUENCY RESPONSES AND THEIR SENSITIVITIES

Type	Response Formula	Expression for Sensitivity w.r.t. ϕ
return loss (common port or channel output port)	$-20 \log_{10}|\rho|$	$c\,\mathrm{Re}\left[\dfrac{\rho_\phi}{\rho}\right]$
transducer loss $\dagger$	$-10 \log_{10}\left(\dfrac{4\,|V^k|^2\,R_S}{R_L^k}\right)$	$c\,\mathrm{Re}\left[\dfrac{(V^k)_\phi}{V^k}\right]$
insertion loss $\dagger$	$-20 \log_{10}\left[\dfrac{|V^k|\,(R_S + R_L^k)}{R_L^k}\right]$	$c\,\mathrm{Re}\left[\dfrac{(V^k)_\phi}{V^k}\right]$
gain slope $\dagger$	$c\,\mathrm{Re}\left[\dfrac{(V^k)_\omega}{V^k}\right]$	$c\,\mathrm{Re}\left[\dfrac{(V^k)_{\phi\omega}}{V^k} - \dfrac{(V^k)_\phi\,(V^k)_\omega}{(V^k)^2}\right]$
group delay $\dagger$	$-\mathrm{Im}\left[\dfrac{(V^k)_\omega}{V^k}\right]$	$-\mathrm{Im}\left[\dfrac{(V^k)_{\phi\omega}}{V^k} - \dfrac{(V^k)_\phi\,(V^k)_\omega}{(V^k)^2}\right]$

$$c = -\frac{20}{\ell n\,10}$$

$\dagger$ between common port and channel k output port
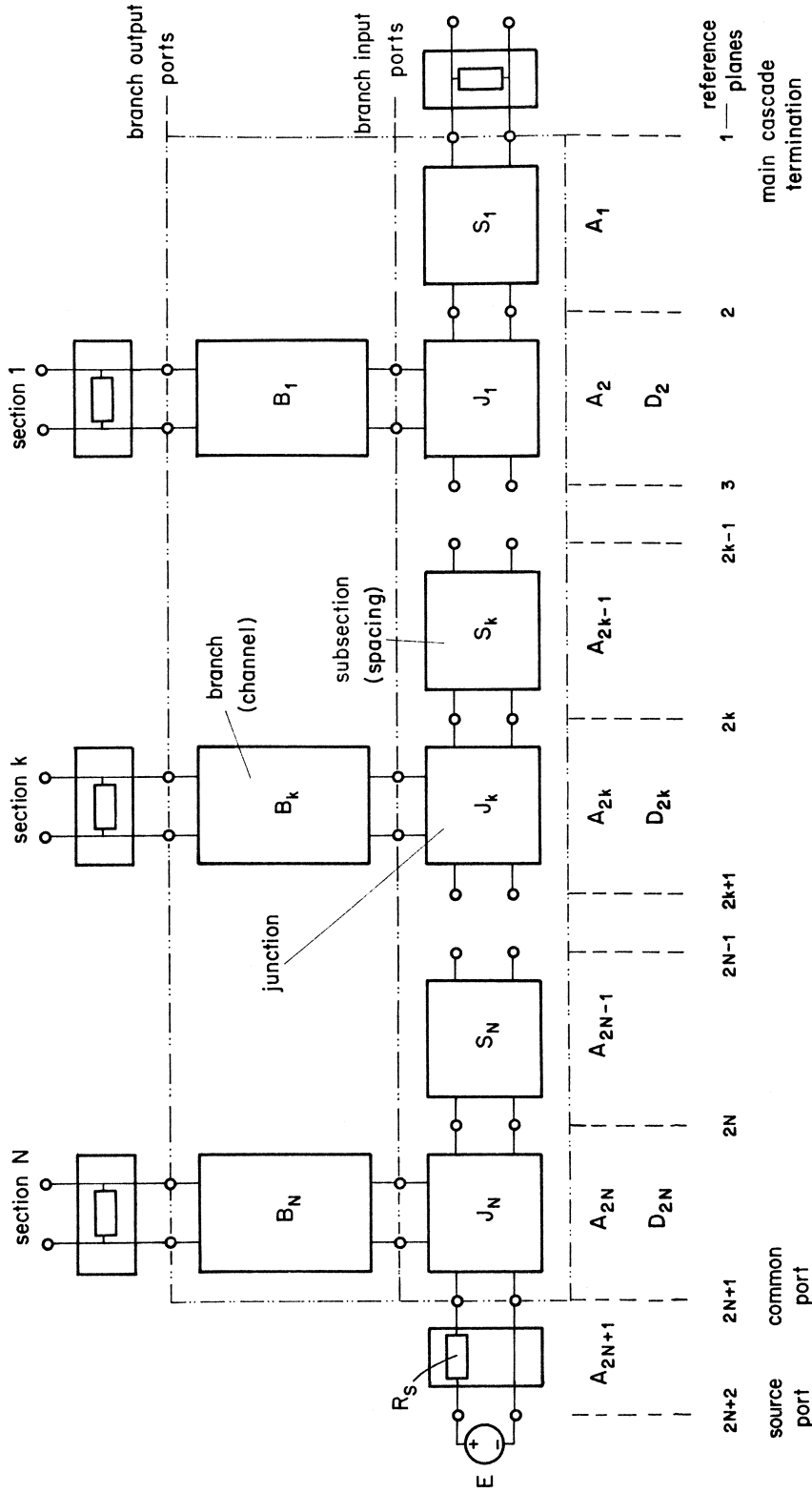
Fig. 1   The branched cascaded network under consideration. J_1, J_2, ..., J_N are arbitrarily defined 3-port junctions. B_1, B_2, ..., B_N are branches or channels which may each be represented in reduced cascade form and S_1, S_2, ..., S_N represent the subsections between junctions. Principal concepts of reference planes, transmission matrices and typical ports are illustrated.
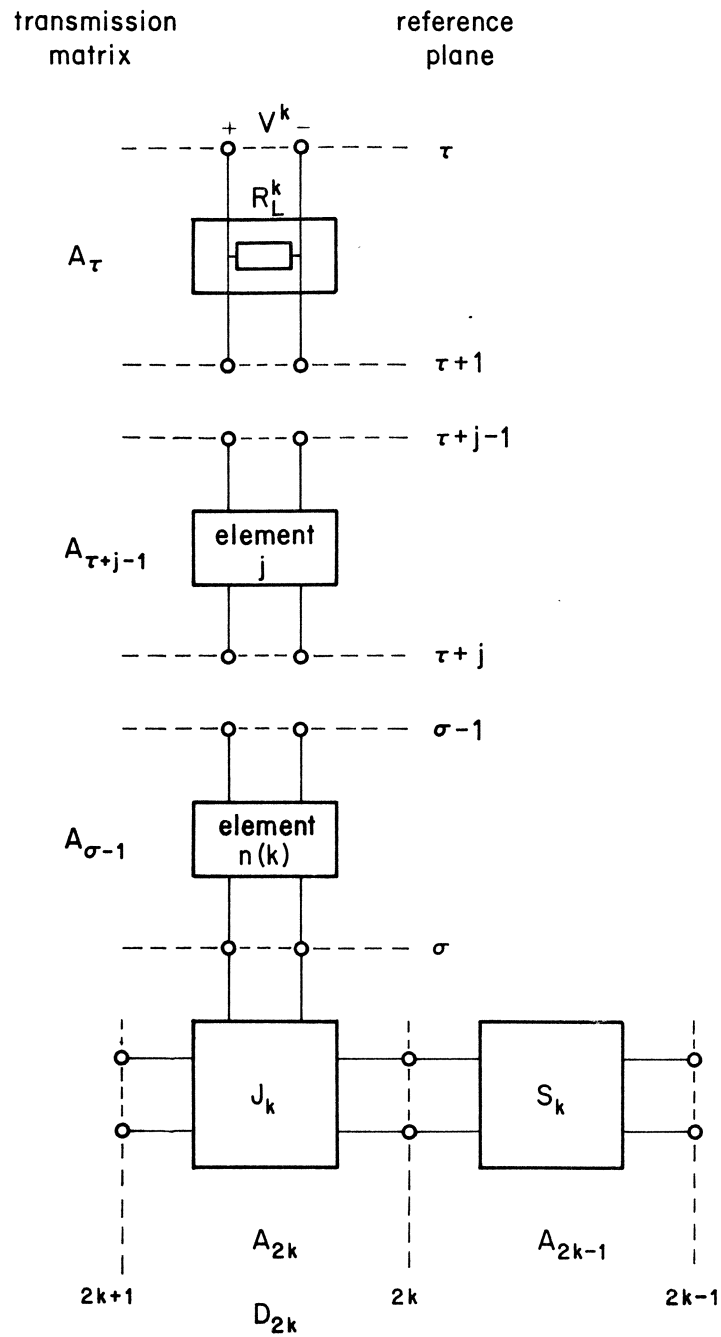
Fig. 2.   Detail of the kth section of a branched cascaded circuit showing reference planes along the branch where $\iota = \iota(k)$ and $\sigma = \sigma(k)$.
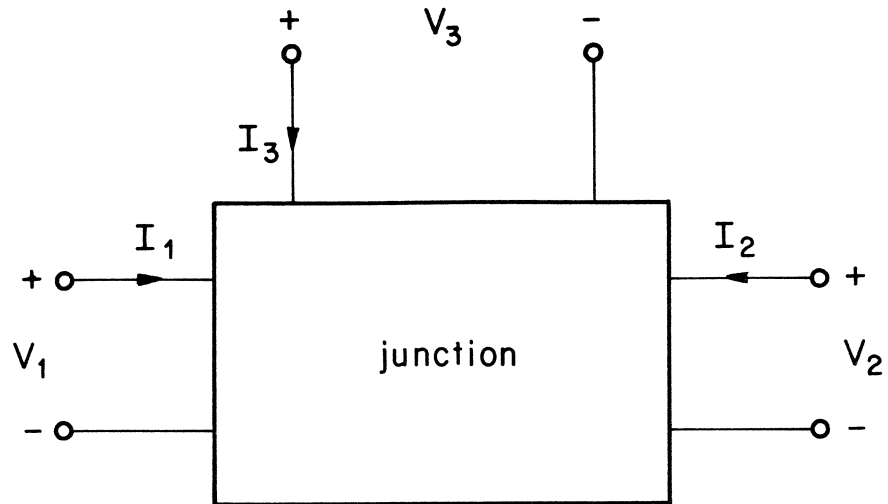
Fig. 3   A 3-port junction in which ports 1 and 2 are considered along a main cascade and port 3 represents a channel or branch of the main cascade.
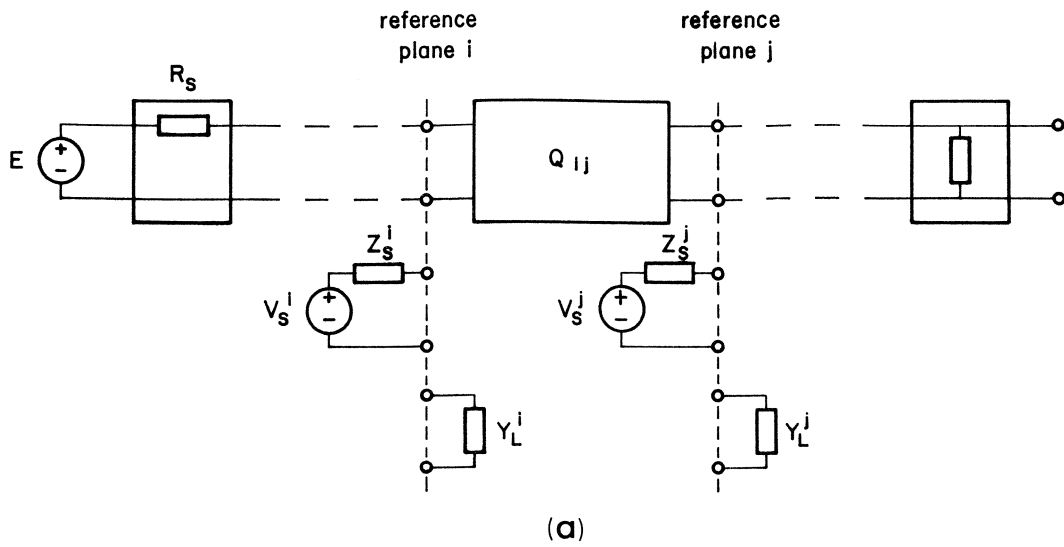
(a)

(b)
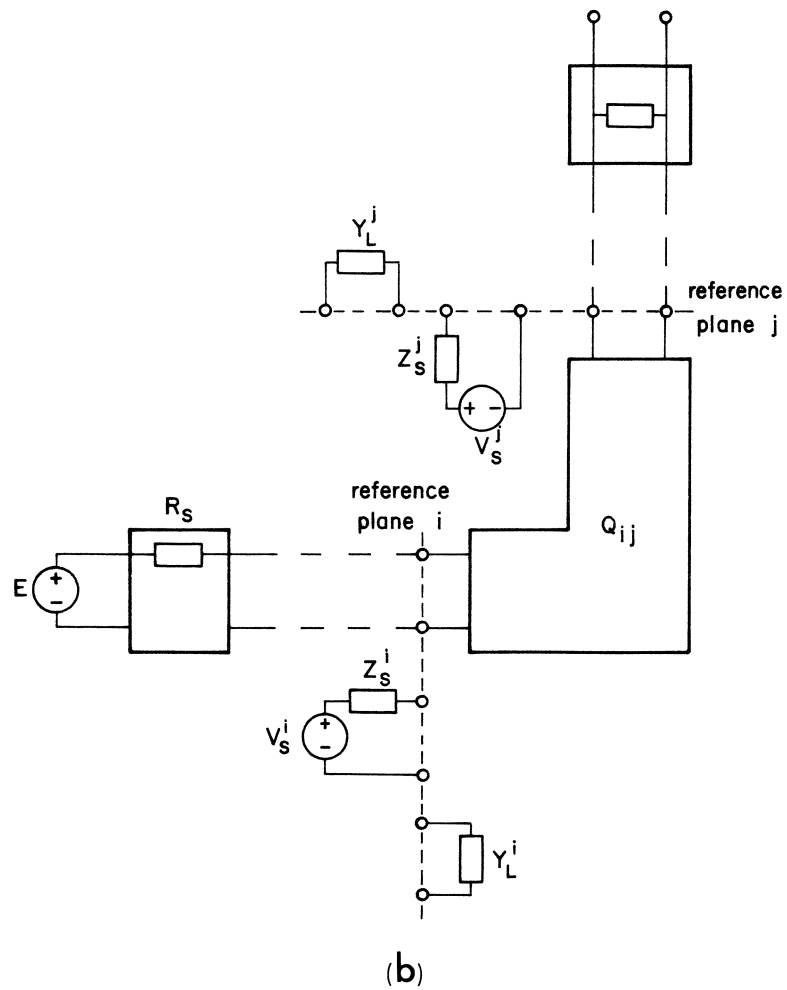
Fig. 4   Thevenin and Norton equivalents at reference planes i and j, where reference plane i is towards the source w.r.t. reference plane j. (a) reference plane j is in the main cascade. (b) reference plane j is in a branch.
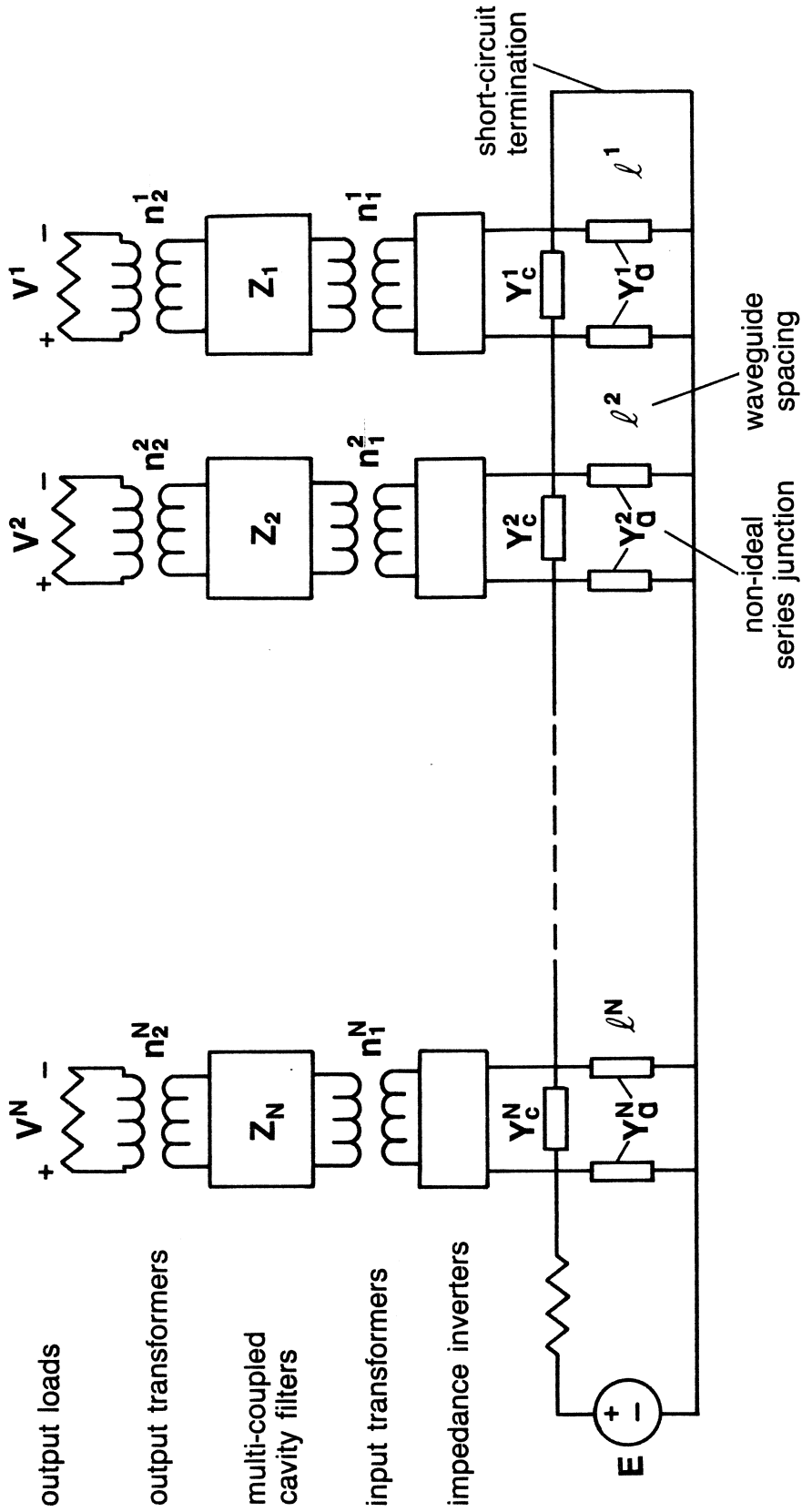
Fig. 5   Equivalent circuit of a contiguous band multiplexer. Each channel has a multi-coupled cavity filter with input and output transformers as well as an impedance inverter. The main cascade is a waveguide manifold with a short circuit termination. Branches are connected to the main cascade through nonideal series junctions.
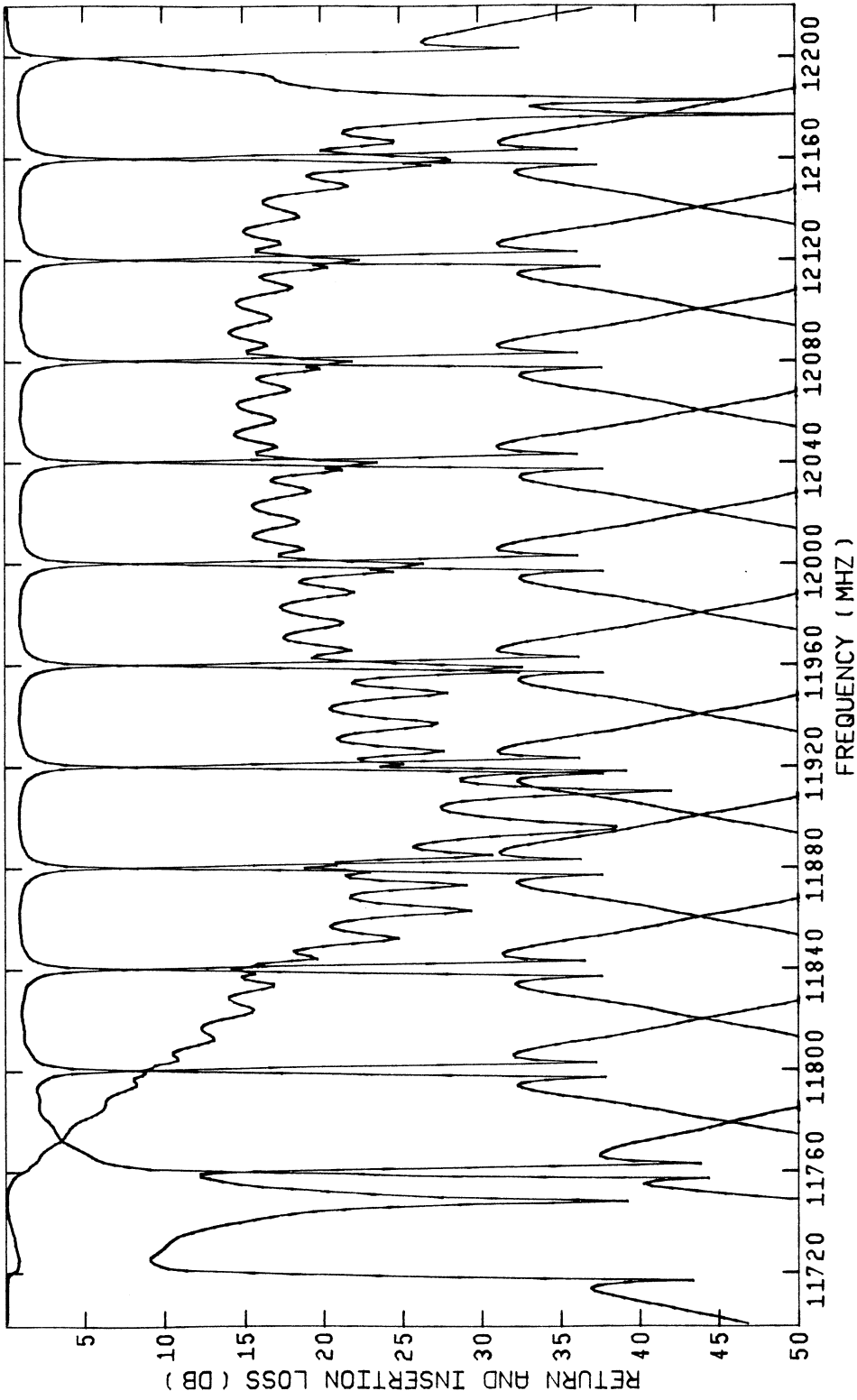
Fig. 6   Common port return loss and channel output port insertion loss responses of the
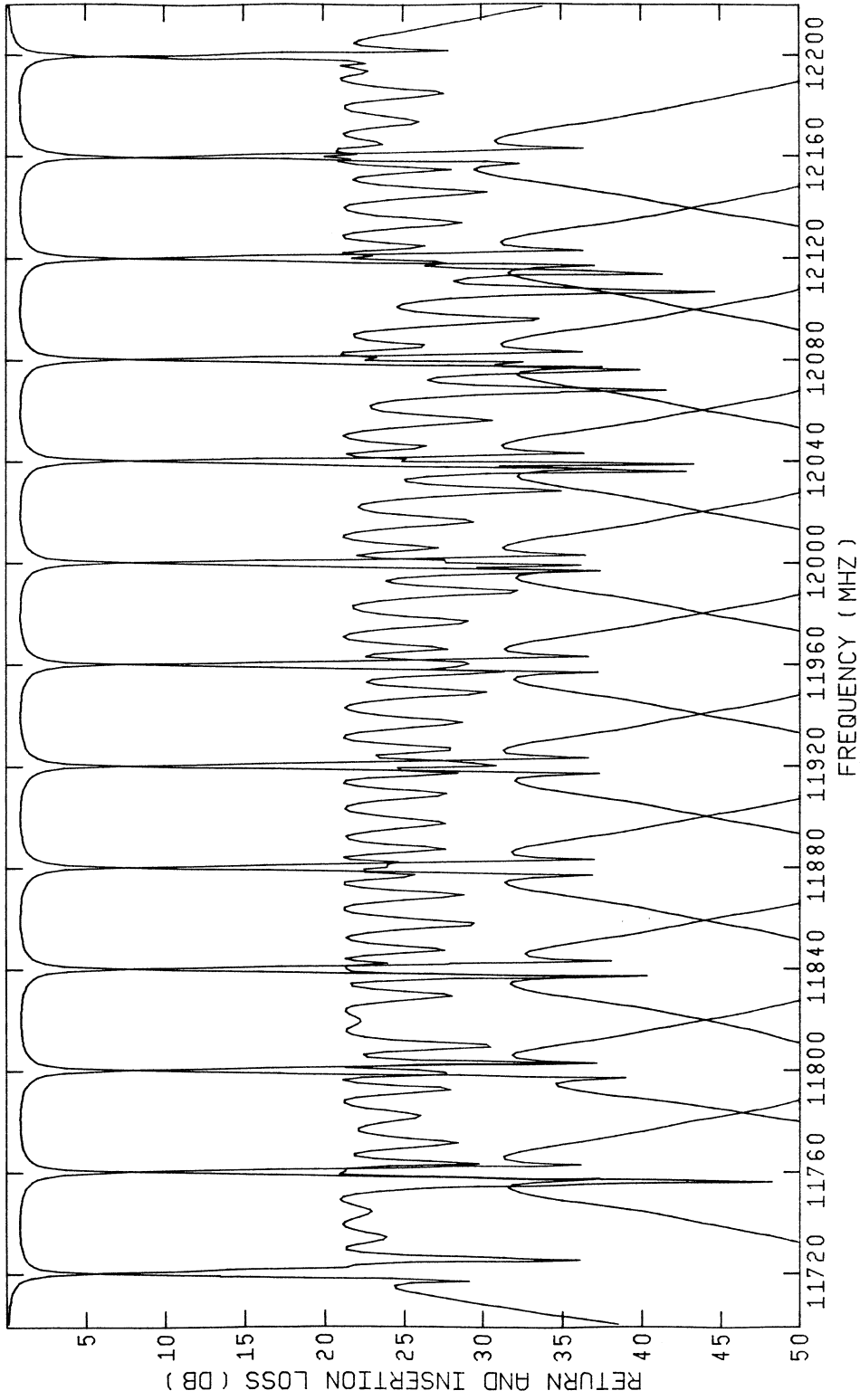12-channel multiplexer before optimization.

Fig. 7   Common port return loss and channel output port insertion loss responses of the
12-channel multiplexer with optimized spacings, input-output transformer
ratios, cavity resonances and coupling parameters.